Mehrnoosh Afshar, Jay Carriere, Tyler Meyer, Ronald Sloboda, Husain Siraj, Nawaid Usmani, Wanyu Liu, Mahdi Tavakoli, Autonomous Ultrasound Scanning to Localize Needle Tip in Breast Brachytherapy, International Symposium on Medical Robotics, Atlanta, USA, 2020.

Autonomous Ultrasound Scanning to Localize Needle Tip in Breast Brachytherapy

Mehrnoosh Afshar[1], Jay Carriere[1], Tyler Meyer[2], Ron Sloboda[3], Siraj Husain[2], Nawaid Usmani[3], Wanyu Liu[1], Mahdi Tavakoli[1]

***Abstract*—The functionality of ultrasound (US) imaging for cancer diagnosis and providing visual assistance for percutaneous therapies has been proven. Clinicians show limited accuracy in performing US imaging, especially for percutaneous therapies, where a needle tip needs to be placed accurately under image guidance. US imaging in the transverse plane is more commonly used in comparison to US imaging in the sagittal plane as what matters more is the position of the needle tip rather than the shape of the entire needle in procedures such as brachytherapy or biopsy. Using a robotic system to perform transverse US image acquisition can enhance the accuracy and repeatability of the imaging and, therefore, help with needle steering. In this paper, an autonomous system for US scanning to help the clinician with localizing and tracking the needle tip is presented. Two strategies to manipulate the probe in synchrony with the needle tip motion are proposed and implemented. As the needle is inserted by the human user, in order to depict the needle tip's deviation from its ideal path for the human user, the ideal needle tip position, which is coincident with one of the guide template's grid points, is dynamically projected on the US image in a real-time fashion. The conducted feasibility study proves the ability of the proposed robotic system to track the needle tip accurately and the helpfulness of the image overlay scheme for guiding the user about the needle tip motion.**

I. Introduction

Percutaneous therapies such as brachytherapy and biopsy, in which a surgeon inserts a surgical needle into the patient's body, have been deployed for diagnosing and treating various cancers such as those of the prostate, breast, and lung [1], [2]. The success of these diagnoses and treatments depends on the accuracy with which the needle is placed with respect to a desired target. If the needle deviates from its desired trajectory, it may not only cause injury to an organ or a blood vessel but also the tip targeting errors can cause misdiagnosis or poor placement of radioactive seeds, giving rise to long-term side effects [3]. Therefore, researchers have worked on robot-assisted needle steering and have considered tissue inhomogeneity [4], tissue anisotropy [5], and target movement [6]–[8] to enhance the needle targeting accuracy. In many of these systems, ultrasound (US) image is the primary feedback to get information about the needle tip location.

Permanent-seed breast brachytherapy is a percutaneous procedure that can be used to irradiate the tissue adjacent to a tumour after the tumour itself has been removed in a procedure called lumpectomy. For this procedure, the general workflow involves first scanning the breast (conventionally, with CT imaging) to create a treatment planning volume. This volume is used to plan the seed implantation locations and radiation dosimetry before the brachytherapy operation. US imaging can be used when performing the needle insertion to provide image guidance about the needle tip position [9]. Imaging repeatability, which relies on the tissue remaining relatively undeformed during imaging and seed implantation, is very important in this workflow to ensure the accuracy of the image-guided needle steering [10]. This requires that the orientation and the position of the US probe with respect to tissue are properly adjusted on a continuous basis to guarantee that the US images adequately capture the needle while ensuring the US probe does not excessively deform the breast.

To achieve this, we propose the use of a robotic US probe holding system. We can design a robot controller to autonomously move the US probe such that it tracks the needle tip position during needle insertion and minimizes breast compression during the scan while maintaining the ultrasound image quality.

The needle imaging can be carried out in the transverse [11], [12] or the sagittal [13]–[15] US imaging plane. The transverse image shows a cross-sectional view of the needle's longitudinal axis. The sagittal image can show a portion of this axis (or all of it if the needle does not undergo considerable 3D bending). In some specific surgeries like permanent prostate brachytherapy, it may not always be possible to capture the needle tip in any arbitrary deflection plane – the needle can deflect in a plane that is not possible to be seen by sagittal imaging. It is simpler to control the US probe position and orientation to always capture the cross-section of the needle tip in transverse plane images as opposed to the sagittal plane [16], [17]. Therefore, in this paper, we focus on tracking the needle tip in transverse images.

This research was supported by the Canada Foundation for Innovation (CFI), the Alberta Innovation and Advanced Education Ministry, the Natural Sciences and Engineering Research Council (NSERC) of Canada, and the Canadian Institutes of Health Research (CIHR).

[1]Mehrnoosh Afshar, Jay Carriere, Wanyu Liu and Mahdi Tavakoli (Corresponding Author) are with the Department of Electrical and Computer Engineering, University of Alberta, AB, Canada T6G 1H9. afsharbo@ualberta.ca, jtcarrie@ualberta.ca, wanyu1@ualberta.ca , mahdi.tavakoli@ualberta.ca

[2]Tyler Meyer and Siraj Husain are with the Division of Radiation Oncology, Tom Baker Cancer Centre, 331 29th Street NW, Calgary, Alberta T2N 4N2. tyler.meyer@albertahealthservices.ca, siraj.husain@albertahealthservices.ca.

[3]Ron Sloboda and Nawaid Usmani are with the Department of Oncology, Cross Cancer Institute, 11560 University Avenue, Edmonton, AB, Canada, T6G 1Z2. nawaid.usmani@albertahealthservices.ca, ron.sloboda@albertahealthservices.ca.

We will consider two different US probe control strategies for keeping the needle tip always visible in transverse US images: A) Orientation control: Rotating the US probe around its contact point with the patient's body surface; B) Translational control: Moving the US probe over the patient's body surface while its orientation is aligned with the vector headed toward the needle tip from the probe contact point. In this paper, we will consider both of these methods. By analyzing the US scanning results, we will confirm the utility of the autonomous breast US scanning system.

In brachytherapy, the needles are inserted through a hole in a square grid (the guide template) into the tissue. The grid hole defines the insertion axis for the needle, and it is crucial to reduce the deflection of the needle tip away from this axis. As the needle is being inserted by the user, we propose the use of a visual overlay of the grid point locations onto the plane of the ultrasound images. This is similar to projection-based Augmented Reality (AR), whose advantage has been proven in other applications such as rehabilitation has been proven [18], [19]. This overlay will aid the user in understanding the deviation of the needle tip from its desired trajectory, which is coincident with a particular grid point position because in brachytherapy, the needles are planned to travel on a straight line. This help with situational awareness is expected to enhance the capability of the user in terms of steering the needle and thus the clinical outcomes. In this paper, we will outline a method to ensure that the grid points are properly projected on these US images for various orientations and positions of the US probe commensurate with the needle insertion.

The paper is organized as follows. Section II provides an outline of the coordinate frames affixed to the ultrasound probe and how orientation control and translational control of the probe work. The gridpoint projection method is introduced in Section III. The experimental setup, procedures, and results are discussed in Section IV. Finally, concluding remarks are provided in Section V.

II. Ultrasound Probe Control

The objectives of the robot controller for the US probe manipulation task are 1) Control of the position and orientation of the US probe to keep the needle tip always visible in transverse US images, 2) Control of the normal force applied by the US probe on the tissue to ensure satisfactory US image quality.

Two coordinate frames will be defined to implement the position and force control of the US probe. The first one is a fixed or base coordinate frame, $\{\mathrm{B}\}$, and the second one is the US probe-affixed coordinate frame, $\{\mathrm{P}\}$. For a curved US probe, the center of the coordinate frame $\{\mathrm{P}\}$ is attached to the center of the imaging arc (Fig. 1). For a flat US probe, the center of the probe coordinate may be selected at any arbitrary distance from the imaging plane (Fig. 1). For the experiments performed in this paper, a flat US probe is used for the experiments, and the center of the probe frame is located in the middle of the US probe surface.

As discussed previously, for the probe orientation control scenario, the main objective is to control the orientation of the probe around a center of rotation. This center of rotation is the centroid of the region where the probe contacts the tissue, and rotating the probe about this point will be used to keep the needle tip visible in the images. In the probe translational control scenario, tracking of the needle tip is done by moving the probe along a line conforming to the surface of the body to keep the needle tip in the imaging plane. In both situations, after adjusting the position and orientation of the US probe, force control is carried out along the Z-axis of the US probe frame, Z_P.

To implement the orientation and translational control, the desired US probe coordinate frames need to be calculated. In the following subsections, the procedure for this step is described.

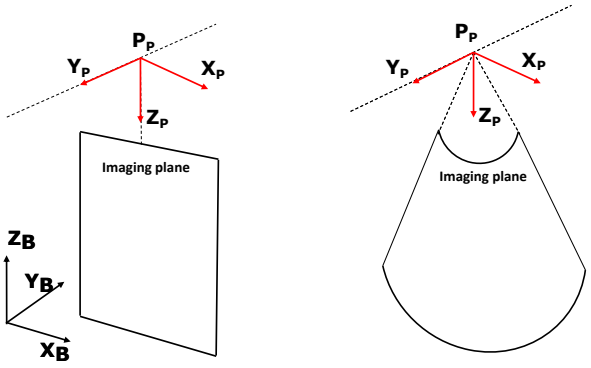

(a) Flat probe. (b) Curved probe.

Figure 1: The ultrasound probe coordinate frame.

A. Orientation Control

The objective of the orientation controller is to rotate the US probe around a virtual center of rotation. The middle point on the scanning head surface of the US probe is selected as the probe rotation center point that is also the origin of the $\{P\}$ frame as shown in Fig. 2.

The desired orientation of the US probe frame needed to enable tracking of the needle tip in the transverse imaging plane can be obtained by defining the desired orientation of its Z-axis represented in the base coordinate frame (Fig. 2). The desired Z-axis of the probe-affixed frame, Z_{Pd}, is in the direction of a vector from the center point of the probe frame, P_P, to the needle tip point, P_t. The US probe should rotate around its rotation center to align its Z-axis with the desired Z-axis. To find the Euler angles of the final desired probe frame, the rotation matrix from the desired probe frame to the base frame, denoted by ${}^B_D R$ where $\{D\}$ is the desired probe frame, is required. ${}^B_D R$ can be obtained through the use of screw theory. The screw axis, s, around which Z_P rotates to reach Z_{Pd}, can be defined through the cross product of Z_P

and Z_{Pd}:

$$s = \frac{Z_P \times Z_{Pd}}{\|Z_P \times Z_{Pd}\|} \tag{1}$$

The angle of rotation, θ_s, is equal to the angle between Z_P and Z_{Pd}:

$$\theta_s = \cos^{-1}\left(\frac{Z_P \cdot Z_{Pd}}{|Z_P|\,|Z_{Pd}|}\right) \tag{2}$$

Having the screw axis and rotation angle, the 3×3 rotation matrix from the desired probe frame $\{D\}$ to the base frame $\{B\}$ can be determined using

$$\mathrm{R}_{\vec{s},\theta_s} = \begin{bmatrix} s_x^2(1-c\theta_s)+c\theta_s & s_x s_y(1-c\theta_s)-s_z s\theta_s & s_x s_z(1-c\theta_s)+s_y s\theta_s \\ s_x s_y(1-c\theta_s)+s_z s\theta_s & s_y^2(1-c\theta_s)+c\theta_s & s_y s_z(1-c\theta_s)-s_x s\theta_s \\ s_x s_z(1-c\theta_s)-s_y s\theta_s & s_y s_z(1-c\theta_s)+s_x s\theta_s & s_z^2(1-c\theta_s)+c\theta_s \end{bmatrix} \tag{3}$$

where s and c stand for *sin* and *cos* functions, respectively. s_x, s_x, and s_x are the components of s. For any given non-singular rotation matrix, the Euler angles can be calculated.

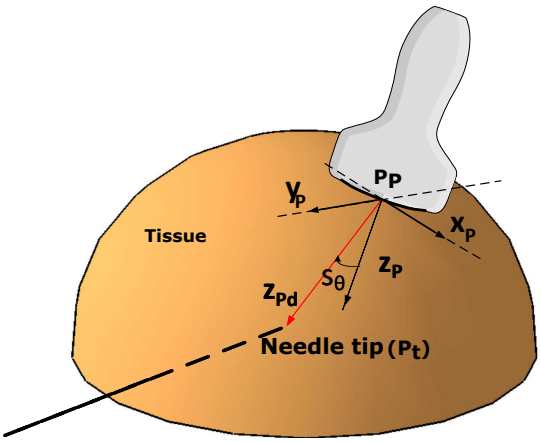

Figure 2: The probe-affixed frame $\{P\}$ and the desired probe frame $\{D\}$ in the probe orientation control scenario.

Having the final Euler angles for the US probe allows for velocity control to be done in a way that rotates the probe around its rotation center to reach and track the desired Euler angles. Force control can be carried out along the final Z-axis of the probe Z_{Pd}. The full control loop is discussed in the section II-C.

B. Translational Control

In the translational control scenario, the probe follows the needle tip by moving over the breast surface while Z_P is aligned with the vector heading toward the needle tip from the probe contact point in the US probe imaging plane. To determine the desired trajectory over the breast surface for the origin of the probe frame P_P to track, we need to define an intersection between a plane $\{\mathrm{N}\}$, defined as containing the longitudinal axis of the needle and the P_P probe contact point, and the breast surface. This problem can be simplified, for real-time control, to one of finding the desired location of the probe P_P corresponding with the current location of the needle tip in a piece-wise fashion instead of finding the whole trajectory.

Based on Fig. 3, the desired location for the tissue-probe contact point, P_{P_d}, can be obtained by finding the intersection between the line perpendicular to the needle axis is the plane $\{\mathrm{N}\}$, denoted by L_N, and the surface of the breast. To determine the breast surface model, the points on the surface of the breast can be captured by any 3D scanner such as Microsoft Kinect. The points captured by the 3D scanner are reported in the frame associated with the 3D scanner, denoted by $\{S\}$. As we require the points in the base frame $\{B\}$, a transformation should be applied to the measured data by the 3D scanner, where ${}^BP = {}^B_S T\,{}^SP$. Having four specified points in frame $\{B\}$ and corresponding points in frame $\{S\}$, transformation matrix ${}^B_S T$ can be calculated. Having the breast surface's points in the base frame, a function can be fit to those points in order to find the approximate shape of the breast. The breast surface model can be defined as $z_{breast} = f(x_{breast}, y_{breast})$, meaning that z_{breast} coordinate of the breast surface is a function of two other independent x_{breast} and y_{breast} coordinates. Given the unit vector of line L_N and the breast surface function $z_{breast} = f(x_{breast}, y_{breast})$, the intersection between the line L_N can be calculated by solving a system of equations.

The desired orientation of the probe is aligned with the line L_N, and the desired Euler angles are calculated in a manner similar to Section II-A. During US scanning, to maintain an adequate force of contact, the probe is pushed downward on tissue parallel to the Z_{Pd} direction for both scenarios.

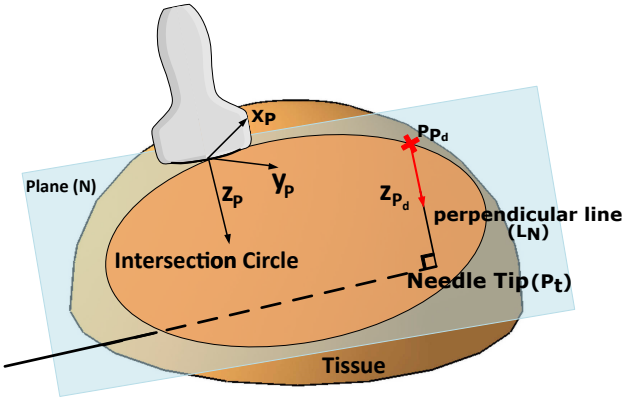

Figure 3: The probe-affixed frame $\{P\}$ and its desired probe position and orientation defined by frame $\{D\}$ in the probe's translational control scenario.

C. Robot Manipulator Controller Design

After defining the desired Cartesian position and orientation of the probe based on what has been discussed in Sections II-A and II-B, the error between the current probe position P_C and orientation $E_{probe} = [\alpha, \beta, \gamma]$ and the desired position and orientation are defined, respectively, as

$$\begin{aligned} e_{\text{Position}} &= P_{P_d} - P_P \\ e_{\text{Euler angle}} &= E_{\text{Desired}} - E_{\text{Probe}} \end{aligned} \tag{4}$$

For Cartesian position control translational probe control, the desired Cartesian velocity of P_P of the probe is given as the control input in the task space:

$$V_{\text{Cartesian}} = K_1 e_{\text{Position}} + K_2 \int_{t_0}^{t} e_{\text{Position}} dt + K_3 \frac{de_{\text{Position}}}{dt} \quad (5)$$

Here, K_1, K_2, and K_3 are PID control gains.

For the orientation control, we desire that the probe rotates around its point of contact with the tissue. An internal position control loop is implemented to guarantee that the probe contact point does not move (i.e., only rotates) with respect to the tissue. A block diagram that explains the orientation control is depicted in Fig. 4. The angular velocity control input is provided by the velocity controller as

$$U_{Euler} = G_1 e_{\text{Euler angle}} + G_2 \int_{t_0}^{t} e_{\text{Euler angle}} dt + G_3 \frac{de_{\text{Euler angle}}}{dt} \quad (6)$$

where G_1, G_2, and G_3 are PID control gains.

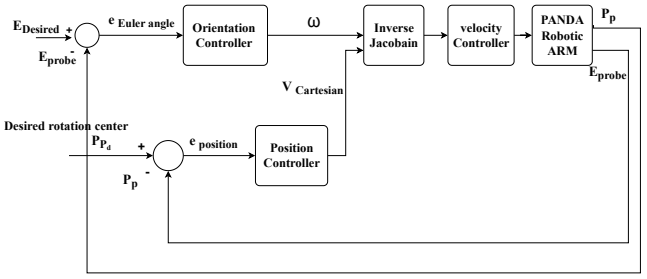

Figure 4: The probe orientation control loop block diagram.

Having the probe at the desired position and orientation, the contact force needs to be adjusted by moving the probe downward on the tissue in the direction of its Z-axis. To define the Cartesian velocity in the probe's Z-axis, a similar velocity controller for force control is implemented, which is shown in Fig. 5. where F_P , F_d, and F_e are applied force

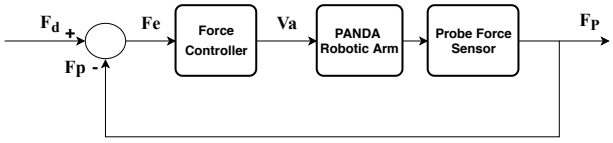

Figure 5: The probe force control loop block diagram.

by the robot to the tissue that is measured by a force sensor, the desired contact force and force error, respectively. V_a is the velocity control input along Z_{Pd}.

III. Grid Points Projection

The goal is to project the guide template's grid points coordinates that are given in the base frame on the US imaging plane by considering the US probe-affixed frame. First, the intersections between the axes of holes in the guide template and the imaging plane are obtained as it is shown in Fig. 6. The intersection points are represented in the base frame $\{B\}$. Therefore, the transformation matrix from the metric base frame $\{B\}$ to the US image's pixel domain is required. In this paper, we are using a flat rectangular ultrasound probe that generates a rectangular image. Therefore, an affine transformation matrix, ${}^P_B T$, is enough to do the point registration. The general form of ${}^P_B T$ is

$${}^P_B T = {}^P_B A \cdot {}^P_B B \cdot {}^P_B C \quad (7)$$

where A is a translation matrix from the origin of one frame to another, B is a rotation matrix that corresponds to the angles between the frames, and C is a scaling matrix that converts the units of one frame to another. The C matrix, which is responsible for scaling real-word domain coordinates to image's pixel domain, is given by

$${}^P_B C = \begin{bmatrix} {}^P_B a_x & 0 & 0 & 0 \\ 0 & {}^P_B a_y & 0 & 0 \\ 0 & 0 & {}^P_B a_z & 0 \\ 0 & 0 & 0 & 1 \end{bmatrix} \quad (8)$$

where ${}^P_B a_x$, ${}^P_B a_y$,and ${}^P_B a_z$ are the pixel domain scaling factors in x, y, and z directions respectively. To obtain the A, B, and C matrices empirically, four points and the clear corresponding points on the ultrasound image are selected. These four points are enough to solve equations ${}^P_B A = {}^P P^B P^{-1}$, ${}^P_B B = {}^P P^B P^{-1}$, and ${}^P_C A = {}^P P^B P^{-1}$ and calculate ${}^P_B T$.

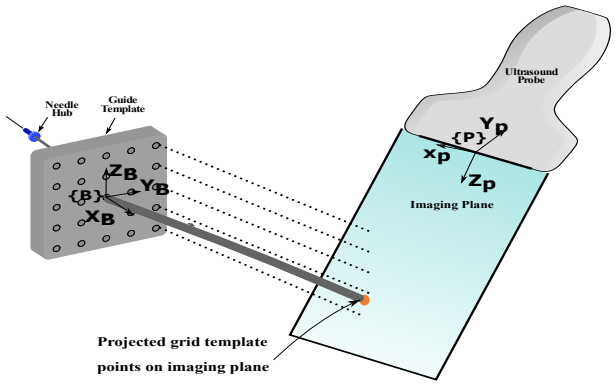

Figure 6: Guide template's points projection on the ultrasound imaging plane.

IV. Experimental Setup and Results

In our experiments, the US probe is connected to an Axia NET force/torque sensor (ATI Industrial Automation, Apex, NC, USA) and is mounted on a Panda robot (Franka Emika GmbH, Munich, Germany) (see Fig. 7). An Ultrasonix Touch US scanner with a 4DL14-5/38 Linear 4D transducer (Analogic Corp, Peabody, MA, USA) is used to obtain the images. Only the 2D imaging functionality of the ultrasound probe is used in these experiments. The Panda robot is driven by a velocity controller. The robot controller is programmed and implemented in Matlab 2019a (The Mathworks Inc, Natwick, MA, USA) and ran using the Simulink Real-Time environment on an Intel Core i7-3930K running at 3.20 GHz (Intel Corporation, Santa Clara, CA, USA). A MicronTracker (Claron Technology Inc, Toronto, Canada) is utilized to track the location of the needle base in one direction. Given the

needle base location and the needle length, the needle tip position can be calculated. The biomimetic tissue used in the experiments is a phantom tissue sample that is created from plastisol (M-F Manufacturing Co, Fort Worth, USA).

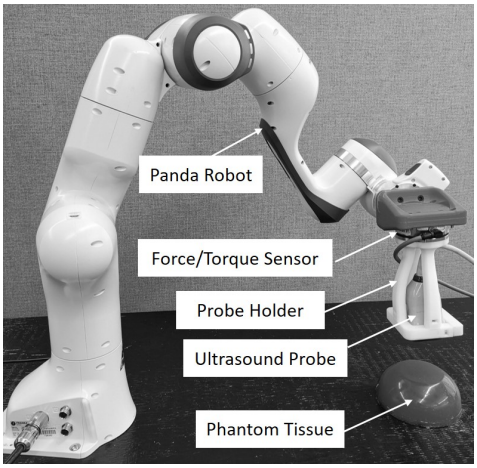

Figure 7: Experimental setup with robot, ultrasound probe, force/torque sensor and phantom tissue.

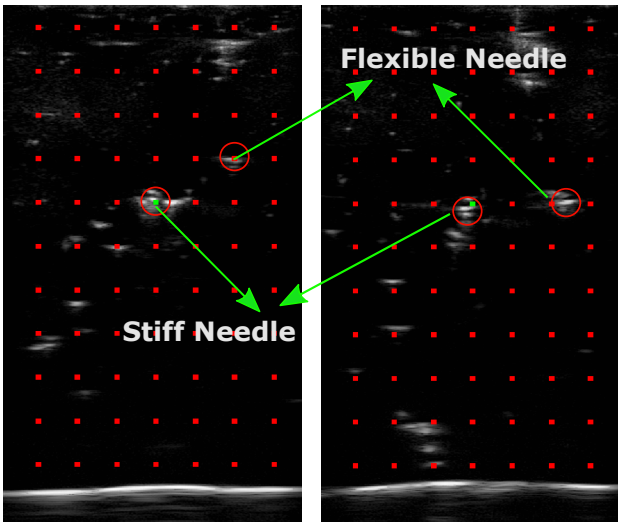

(a) The US image at the beginning of the needle insertion (b) The US image at the middle of the needle insertion

Figure 8: The US images captured through the needle insertion.

The experiments include four scenarios to evaluate the assistive effect of autonomous US scanning and visual projection on the needle tip localization. The NASA Task Load Index (NASA-TLX) experiment is carried out on five participants to assess the performance of the proposed robotic system. Each participant does the insertion once for each of the four scenarios. Those four scenarios are as follows:

Scenario 1) The translational controller will drive the US probe to track the needle tip during needle insertion, and the grid template points will NOT be projected on the US image,

Scenario 2) The translational controller will drive the US probe to track the needle tip during needle insertion, and the grid template points will be projected on the US image,

Scenario 3) The orientation controller will drive the US probe to track the needle tip during needle insertion, and the grid template points will NOT be projected on the US image,

Scenario 4) The orientation controller will drive the US probe to track the needle tip during needle insertion, and the grid template points will be projected on the US image,

In Fig. 8a and Fig. 8b, the guide template projection onto two US images captured during the translational control at the beginning and the middle of needle insertion are shown. The hypothesis is that such an image overlay helps the user track the needle tip deviation from the ideal position. A stiff needle serves as a (relatively) fixed visual marker while a flexible brachytherapy needle is what is to be traced by the user.

A. *Experiment Results and Analysis*

The participants for the user trial were engineering students with little to no familiarity with US scanning and percutaneous therapies. For each of the four scenarios, the participants were asked to insert the needle into the tissue, to follow the needle tip in the ultrasound images, and to predict the approximate deviation of the needle tip from its desired location. For all of the scenarios, the participants were allowed to use their dominant hand, and the insertion velocity of the needle was not controlled. The participants were asked to rate the difficulty of each scenario using three criteria from the standard NASA-TLX evaluation, where the three criteria of interest are the performance, effort, and frustration of the system. For the four scenarios, performance means how successful the user feels in predicting the approximate location of the needle tip by using the proposed robotics system (i.e. how well they thought they could estimate needle deflection in each of the four scenarios). The effort and frustration measure how hard this needle localization task is for the user and how unconfident the user is about the final result of the task. For each of the four scenarios, participants were asked to answer the NASA-TLX-based questionnaire by rating each of the three aspects on a 20-point Likert Scale (i.e. very low=1, very high=20).

The results for the NASA-TLX usability criteria, for each scenario, are displayed in Fig. 9. The mean and variance of results for each criterion are given in Table I. Based on the results provided in Table I, the performance in Scenarios 2 and 4 (when the visualization overlay is applied) is higher than Scenarios 1 and 3 (where no overlay is provided). The averaged results for the usability of Scenario 1 thorough Scenario 4 are shown in Fig. 9.

In order to evaluate if the changing parameters between various scenarios (i.e. the control strategies and grid point visualization) significantly affect the resultant data, a T-test analysis is carried out. The T-test analysis, reported in Table II, returns a T-test decision logic which is a 1 (i.e. P-value

Table I: Statistics results of the experiment averaged across all users.

Scenario	Statistics	NASA-TLX		
		Performance	Effort	Frustration
1	Mean	8.4	10.4	12.6
	Variance	2.4	3.5	2.4
2	Mean	15.6	5	5.4
	Variance	1.3	1.5	1.1
3	Mean	9.8	10	11.8
	Variance	1.3	3	1.7
4	Mean	14	5.8	5.8
	Variance	1.4	2.5	1.6

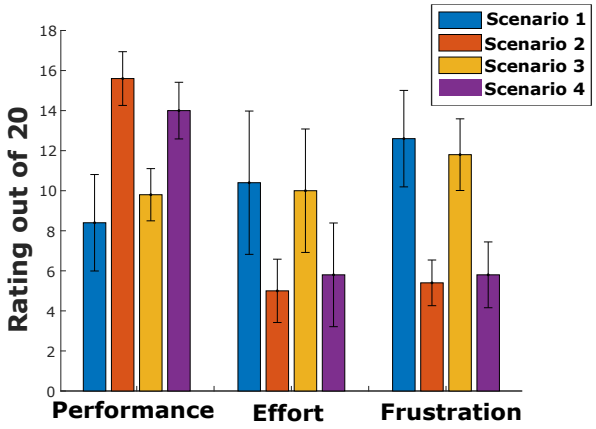

Figure 9: NASA-TLX result for the four sets of experiments.

less than 0.05) if the average user performance between the two Scenarios is statistically meaningful and a 0 (i.e. P-value greater than 0.05) if there is no statistical difference between the performance in the two Scenarios. Table II shows the T-test result between every two possible Scenarios. Based on Table II, there is a meaningful difference between the result of Scenarios 1 and 2, and also between Scenarios 3 and 4, which means that the image overlay significantly enhances the performance and ease with which the user is able to complete the needle tracking task.

However, there is no statistically significant difference between Scenario 1 and Scenario 3 that reveals the two different strategies for probe control do not significantly affect user performance. One thing to note is that the orientation control strategy faces a geometric limitation (due to poor probe/tissue contact at large angles) when tracking the needle tip, and therefore the workspace of the orientation controller was limited in order to maintain contact between the probe and the tissue (at an angle less than 40 degrees in our experiments). The only advantage of the translational control strategy, over the rotational control strategy, is that it could track the needle tip without being limited by geometry; however, it has the disadvantage of causing more tissue deformation as the probe is moved.

V. Conclusion

An autonomous ultrasound scanning system was proposed in this paper. The objective of the system is to track and visualize for the user the needle tip position in the tissue during the needle insertion. Two control strategies (translational and orientation probe control strategy) were suggested, and the feasibility of those for the needle tip tracking was investigated. To increase the capability of the user to estimate the needle tip deviation from the desired path, the guide template's grid points, which are coincident with the desired needle tip positions, were projected on the US image in a real-time fashion. A usability study was performed by doing the NASA-TLX evaluation of five participants. The result of NASA-TLX evaluation has shown that the performance of probe control with guide template points projection on the US image is higher in comparison to the probe control without guide template points projection. This means that the proposed image overlay is helpful for the user and increases their awareness about the needle tip location, which is essential for keeping the needle targeting errors low. The user is not able to feel a difference between the translational and orientation probe control methods. The probe range of motion is limited for orientation control as the contact between the tissue, and the probe cannot be maintained for a high degree of probe rotation. On the other hand, the orientation control approach has the advantage of causing less deformation to the tissue.

Table II: T-test results.

Scenario	1	2	3	4
1	-	1 (P-value=0.0004)	0 (P-value=0.2861)	1 (P-value=0.002)
2	1 (P-value=0.0004)	-	1 (P-value=0.001)	0 (P-value=0.1038)
3	0 (P-value=0.2861)	1 (P-value=0.001)	-	1 (P-value=0.0012)
4	1 (P-value=0.002)	0 (P-value=0.1038)	1 (P-value=0.001)	-

References

[1] N. J. Cowan, K. Goldberg, G. S. Chirikjian, G. Fichtinger, R. Alterovitz, K. B. Reed, V. Kallem, W. Park, S. Misra, and A. M. Okamura, *Robotic Needle Steering: Design, Modeling, Planning, and Image Guidance*. Boston, MA: Springer US, 2011, pp. 557–582.

[2] C. Rossa and M. Tavakoli, "Issues in closed-loop needle steering," *Control Engineering Practice*, vol. 62, pp. 55 – 69, 2017.

[3] I. M. Buzurovic, S. Salinic, P. F. Orio, P. L. Nguyen, and R. A. Cormack, "A novel approach to an automated needle insertion in brachytherapy procedures," *Medical & Biological Engineering & Computing*, vol. 56, no. 2, pp. 273–287, Feb 2018.

[4] C. Rossa, T. Lehmann, R. Sloboda, N. Usmani, and M. Tavakoli, "A data-driven soft sensor for needle deflection in heterogeneous tissue using just-in-time modelling," *Medical & Biological Engineering & Computing*, vol. 55, no. 8, pp. 1401–1414, Aug 2017.

[5] W. Liu, Z. Yang, and S. Jiang, "A mechanics-based model for simulating the needle deflection in transverse isotropic tissue for a percutaneous puncture," *Journal of Mechanics in Medicine and Biology*, vol. 19, no. 06, p. 1950060, 2019.

[6] G. J. Vrooijink, M. Abayazid, S. Patil, R. Alterovitz, and S. Misra, "Needle path planning and steering in a three-dimensional non-static environment using two-dimensional ultrasound images," *The International Journal of Robotics Research*, vol. 33, no. 10, pp. 1361–1374, 2014.

[7] J. Chevrie, N. Shahriari, M. Babel, A. Krupa, and S. Misra, "Flexible needle steering in moving biological tissue with motion compensation using ultrasound and force feedback," *IEEE Robotics and Automation Letters*, vol. 3, no. 3, pp. 2338–2345, July 2018.

[8] J. Chevrie, A. Krupa, and M. Babel, "Online prediction of needle shape deformation in moving soft tissues from visual feedback," in

2016 IEEE/RSJ International Conference on Intelligent Robots and Systems (IROS), Oct 2016, pp. 2375–2380.

[9] M. Khadem, C. Rossa, N. Usmani, R. S. Sloboda, and M. Tavakoli, "Semi-automated needle steering in biological tissue using an ultrasound-based deflection predictor," *Annals of Biomedical Engineering*, vol. 45, no. 4, pp. 924–938, Apr 2017.

[10] J. Carriere, J. Fong, T. Meyer, R. Sloboda, S. Husain, N. Usmani, and M. Tavakoli, "An admittance-controlled robotic assistant for semi-autonomous breast ultrasound scanning," in *2019 International Symposium on Medical Robotics (ISMR)*, April 2019, pp. 1–7.

[11] P. Moreira and S. Misra, "Biomechanics-based curvature estimation for ultrasound-guided flexible needle steering in biological tissues," *Annals of Biomedical Engineering*, vol. 43, no. 8, pp. 1716–1726, Aug 2015.

[12] M. Abayazid, G. J. Vrooijink, S. Patil, R. Alterovitz, and S. Misra, "Experimental evaluation of ultrasound-guided 3d needle steering in biological tissue," *International Journal of Computer Assisted Radiology and Surgery*, vol. 9, no. 6, pp. 931–939, Nov 2014.

[13] S. H. Okazawa, R. Ebrahimi, J. Chuang, R. N. Rohling, and S. E. Salcudean, "Methods for segmenting curved needles in ultrasound images," *Medical image analysis*, vol. 10, no. 3, pp. 330–342, 2006.

[14] M. Kaya and O. Bebek, "Needle localization using gabor filtering in 2d ultrasound images," in *2014 IEEE International Conference on Robotics and Automation (ICRA)*, 2014, pp. 4881–4886.

[15] J. Carriere, C. Rossa, N. Usmani, R. Sloboda, and M. Tavakoli, "Needle shape estimation in soft tissue based on partial ultrasound image observation," in *2015 IEEE International Conference on Robotics and Automation (ICRA)*. IEEE, 2015, pp. 2277–2282.

[16] M. Waine, C. Rossa, R. Sloboda, N. Usmani, and M. Tavakoli, "Needle tracking and deflection prediction for robot-assisted needle insertion using 2d ultrasound images," *Journal of Medical Robotics Research*, vol. 01, p. 1640001, 03 2016.

[17] M. Khadem, C. Rossa, R. S. Sloboda, N. Usmani, and M. Tavakoli, "Ultrasound-guided model predictive control of needle steering in biological tissue," *Journal of Medical Robotics Research*, vol. 1, no. 01, p. 1640007, 2016.

[18] R. Ocampo and M. Tavakoli, "Visual-haptic colocation in robotic rehabilitation exercises using a 2d augmented-reality display," in *2019 International Symposium on Medical Robotics (ISMR)*. IEEE, 2019, pp. 1–7.

[19] J. Fong, R. Ocampo, D. P. Gros, and M. Tavakoli, "A robot with an augmented-reality display for functional capacity evaluation and rehabilitation of injured workers," in *2019 IEEE 16th International Conference on Rehabilitation Robotics (ICORR)*. IEEE, 2019, pp. 181–186.